

Comparison of the Binding of 3-Fluoromethyl-7-sulfonyl-1,2,3,4-tetrahydroisoquinolines with Their Isosteric Sulfonamides to the Active Site of Phenylethanolamine *N*-Methyltransferase¹

Gary L. Grunewald,*[‡] Mitchell R. Seim,[†] Rachel C. Regier,[†] Jennifer L. Martin,[‡] Christine L. Gee,[‡] Nyssa Drinkwater,[‡] and Kevin R. Criscione[†]

Department of Medicinal Chemistry, University of Kansas, Lawrence, Kansas 66045, and Institute for Molecular Bioscience and Special Research Centre for Structural and Functional Genomics, University of Queensland, Brisbane, Queensland 4072, Australia

Received April 19, 2006

3-Fluoromethyl-7-(*N*-substituted aminosulfonyl)-1,2,3,4-tetrahydroisoquinolines (**14**, **16**, and **18–22**) are highly potent and selective inhibitors of phenylethanolamine *N*-methyltransferase (PNMT). Molecular modeling studies with 3-fluoromethyl-7-(*N*-alkyl aminosulfonyl)-1,2,3,4-tetrahydroisoquinolines, such as **16**, suggested that the sulfonamide –NH– could form a hydrogen bond with the side chain of Lys57. However, SAR studies and analysis of the crystal structure of human PNMT (hPNMT) in complex with **7** indicated that the sulfonamide oxygens, and not the sulfonamide –NH–, formed favorable interactions with the enzyme. Thus, we hypothesized that replacement of the sulfonamide –NH– with a methylene group could result in compounds that would retain potency at PNMT and that would have increased lipophilicity, thus increasing the likelihood they will cross the blood brain barrier. A series of 3-fluoromethyl-7-sulfonyl-1,2,3,4-tetrahydroisoquinolines (**23–30**) were synthesized and evaluated for their PNMT inhibitory potency and affinity for the α_2 -adrenoceptor. A comparison of these compounds with their isosteric sulfonamides (**14**, **16**, and **18–22**) showed that the sulfones were more lipophilic but less potent than their corresponding sulfonamides. Sulfone **24** (hPNMT $K_i = 1.3 \mu\text{M}$) is the most potent compound in this series and is quite selective for PNMT versus the α_2 -adrenoceptor, but **24** is less potent than the corresponding sulfonamide, **16** (hPNMT $K_i = 0.13 \mu\text{M}$). We also report the crystal structure of hPNMT in complex with sulfonamide **15**, from which a potential hydrogen bond acceptor within the hPNMT active site has been identified, the main chain carbonyl oxygen of Asn39. The interaction of this residue with the sulfonamide –NH– is likely responsible for much of the enhanced inhibitory potency of the sulfonamides versus the sulfones.

Introduction

Epinephrine accounts for approximately 5% of the total catecholamine content in the mammalian central nervous system (CNS),^{2–4} however, its role therein is not well-understood.⁵ Based largely on CNS localization, epinephrine neurons are thought to be involved in the regulation of blood pressure, respiration, and body temperature,⁶ the secretion of hormones from the pituitary gland,⁷ the regulation of α_2 -adrenoceptors in the hypothalamus,⁸ and some of the neurodegeneration seen in Alzheimer's disease.^{9–11} As one approach to study the effects of epinephrine in the CNS, our laboratory has targeted phenylethanolamine *N*-methyltransferase (PNMT; EC 2.1.1.28). This enzyme catalyzes the terminal step in the biosynthesis of epinephrine (Figure 1) in which an activated methyl group is transferred from *S*-adenosyl-L-methionine (AdoMet; **3**) to the primary amine of norepinephrine (**1**) to form epinephrine (**2**) and the cofactor product *S*-adenosyl-L-homocysteine (AdoHcy; **4**).

The most thoroughly studied physiological process to which epinephrine in the CNS has been linked is the regulation of peripheral blood pressure. Administration of the PNMT inhibitor **5** (SK&F 64139,¹² Table 1) to hypertensive rats resulted in a reduction in blood pressure.¹³ However, like many of the previously studied 1,2,3,4-tetrahydroisoquinoline (THIQ, **6**) inhibitors of PNMT, **5** was nonselective due to significant

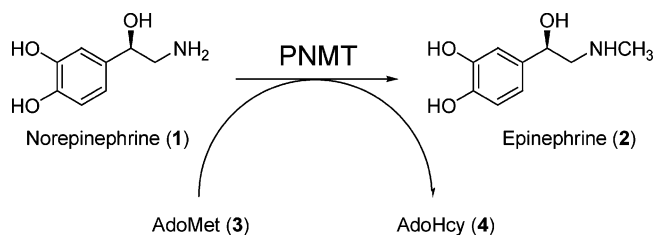


Figure 1. Terminal step in epinephrine (**2**) biosynthesis is the transfer of a methyl group from AdoMet (**3**) to norepinephrine (**1**) to form epinephrine (**2**) and the cofactor product AdoHcy (**4**).

affinity for the α_2 -adrenoceptor.¹⁴ Thus, some of the decrease in blood pressure may be attributed to an α_2 -adrenergic effect rather than to decreases in CNS epinephrine concentrations.^{15–17} A potent inhibitor of PNMT, which exhibits minimal affinity for the α_2 -adrenoceptor, would be a useful pharmacological tool for clearly defining the connection between central epinephrine concentrations and blood pressure.

Compound **7** (SK&F 29661)¹⁸ is a selective PNMT inhibitor. Prior to the availability of the X-ray crystal structure of PNMT, a study on a series of THIQ-7-sulfonamides concluded that the acidic –NH– was essential for their PNMT inhibitory activity.¹⁹ However, SAR analysis of a diverse set of compounds indicated that the acidic –NH– was not required for high PNMT inhibitory potency of THIQ-type inhibitors.²⁰ Based on this study, a small series of 7-sulfonyl-THIQs (**8–11**) were prepared and evaluated.²¹ The inhibitory potency of **8** versus that of **7** provided further evidence that the sulfonamide –NH– was not essential for high potency at PNMT.

* To whom correspondence should be addressed. Phone: (785) 864-44970. Fax: (785) 864-5326. E-mail: ggrunewald@ku.edu.

[†] University of Kansas.

[‡] University of Queensland.

Table 1. In Vitro Human PNMT (hPNMT) and α_2 -Adrenoceptor Affinity of Some PNMT Inhibitors

compd	R ⁷	R ⁸	R ³	K_i (μM) \pm SEM ^a		selectivity α_2/hPNMT	ClogP ^c
				hPNMT	α_2^b		
5 ^d	Cl	Cl	H	0.0031 \pm 0.0006 ^e	0.021 \pm 0.005	6.8	2.59
6 ^f	H	H	H	5.8 \pm 0.5	0.35 \pm 0.11	0.060	1.55
7 ^g	SO ₂ NH ₂	H	H	0.28 \pm 0.02 ^e	100 \pm 10	360	0.19
8 ^h	SO ₂ CH ₃	H	H	0.79 \pm 0.02	160 \pm 10	200	0.50
9 ^h	SO ₂ Ph	H	H	23 \pm 3	21 \pm 1	1.1	2.38
10 ^h	SO ₂ CH ₂ CH=CH ₂	H	H	9.0 \pm 0.7	95 \pm 2	11	1.31
11 ^h	SO ₂ CCl ₃	H	H	6.3 \pm 0.6	34 \pm 1	5.4	3.00
12 ⁱ	SO ₂ NH ₂	H	CH ₂ F	0.15 \pm 0.01 ^j	680 \pm 10	4500	0.42
13 ^k	SO ₂ NH ₂	H	CH ₂ OH	0.052 \pm 0.004 ^l	1400 \pm 200	27 000	-0.19
14 ⁱ	SO ₂ NH(4-Cl-Ph)	H	CH ₂ F	0.27 \pm 0.02 ^e	140 \pm 20	520	2.86
15 ^l	SO ₂ NH(4-Cl-Ph)	H	CH ₂ OH	0.063 \pm 0.002	53 \pm 5	840	2.26
16 ^j	SO ₂ NHCH ₂ CF ₃	H	CH ₂ F	0.13 \pm 0.02	1200 \pm 100	9200	1.64
17 ^l	SO ₂ NHCH ₂ CF ₃	H	CH ₂ OH	0.023 \pm 0.002	340 \pm 40	15 000	1.04

^a Standard error of the mean. ^b In vitro activities for the inhibition of [³H]clonidine binding to the α_2 -adrenoceptor. ^c Reference 37. ^d Reference 12. ^e Reference 34. ^f Reference 49. ^g Reference 18. ^h Reference 21. ⁱ Reference 23. ^j Reference 27. ^k Reference 24. ^l Reference 28.

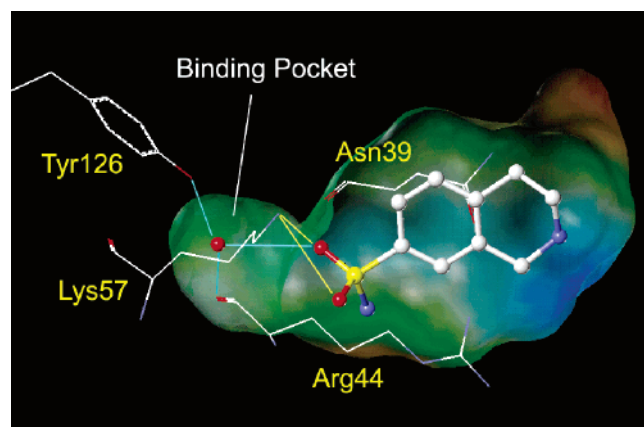


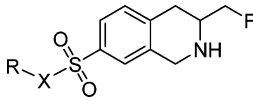
Figure 2. Active site of hPNMT cocrystallized with **7**.²² A Connolly (solvent accessible) surface exposing **7** is also shown and indicates the presence of a binding pocket adjacent to the sulfonamide group of **7**. A lipophilic potential is mapped on the Connolly surface, whereby the areas shown in green are neutral, blue are hydrophilic, and brown are lipophilic. Hydrogen bonds between the sulfonamide oxygens of **7** and Lys57 are shown in yellow. Water-mediated hydrogen bonds between one of the sulfonamide oxygens, the side chain of Tyr126, and the main chain carbonyl oxygen of Arg44 are shown in cyan. Carbon is white, nitrogen is blue, oxygen is red, and sulfur is yellow. Hydrogens are not shown for clarity.

The X-ray crystal structure of human PNMT (hPNMT) cocrystallized with **7** and **4** (hPNMT·**7**·**4**, Figure 2) also supported this hypothesis, because the sulfonamide $-\text{NH}_2-$ of **7** does not appear to form favorable interactions with the enzyme.²² The hPNMT·**7**·**4** structure indicated that the increased inhibitory potency of **7** versus **6** was due to a hydrogen bond between both sulfonamide oxygens and the side chain of Lys57 (Figure 2).²² Also, one of the sulfonamide oxygens makes a water-mediated hydrogen bond with the main chain carbonyl oxygen of Arg44 and the side chain of Tyr126. The importance of the sulfonamide oxygens, and not the $-\text{NH}-$, was consistent with the PNMT inhibitory potency of **8** being very similar to that of **7**.

Prior to the availability of the X-ray crystal structure of PNMT, the addition of a fluoromethyl group (**12**)²³ or hydroxymethyl group (**13**)²⁴ to the 3-position of **7** was found to increase both potency and selectivity for PNMT. However, these compounds are not likely to penetrate the blood brain barrier

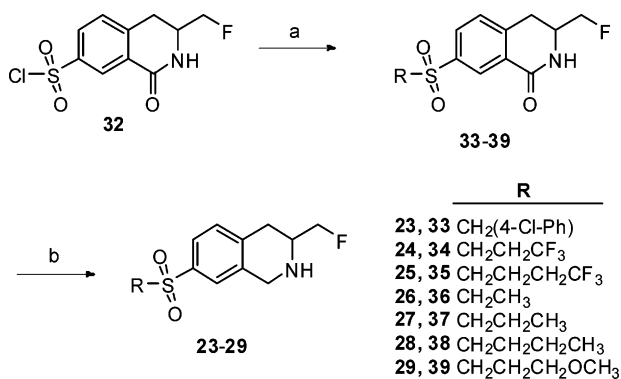
(BBB) as a result of the high polarity of the 7-aminosulfonyl substituent. According to an in vitro BBB model of THIQ-type inhibitors,^{25,26} there is a correlation between increased calculated log P (ClogP) values and their likelihood of BBB penetration.²³ To increase the lipophilicity of **12** or **13**, nonpolar substituents were added to the sulfonamide nitrogen.²⁷ This study was successful in that some of the resulting sulfonamides, such as **14**–**17**,^{27,28} were more lipophilic and virtually equipotent to their parent compounds (**12** and **13**). Docking studies suggested that **14**–**17** retained PNMT inhibitory potency because the substituents on the sulfonamide could occupy a binding pocket adjacent to the sulfonamide group of **7** (Figure 2).^{27,28} In addition to **14** and **16**, a library consisting of a wide variety of 3-fluoromethyl-7-(*N*-alkyl or *N*-aryl aminosulfonyl)-THIQs was prepared and evaluated at PNMT.²⁷ Docking studies and SAR analysis of these compounds allowed us to probe the active site surrounding the sulfonamide group of **7** (Figure 2). From the docking results it appeared that, unlike compound **7**, the sulfonamide $-\text{NH}-$ of substituted sulfonamides could be forming favorable interactions with Lys57.²⁷ Despite this observation, on the overall basis of crystallographic molecular modeling and SAR data (particularly since sulfone **8** was less than 3-fold less-potent than sulfonamide **7**), we proposed that replacement of the sulfonamide $-\text{NH}-$ in a series of highly potent sulfonamide PNMT inhibitors (**14**, **16**, and **18**–**22**, Table 2) with a methylene group would result in compounds (**23**–**30**, Table 2) that would retain PNMT inhibitory potency. By substituting the polar $-\text{NH}-$ group with a methylene group, the resulting 7-alkylsulfonyl-3-fluoromethyl-THIQs would be more lipophilic than the corresponding sulfonamides, thus increasing the likelihood they will cross the BBB.

Chemistry. Sulfonyl chloride **32** was a common starting material that could be used to obtain the desired sulfones and was obtained according to previously described methods.²³ Sulfonyl chloride **32** was converted to sulfones **33**–**39** according to a two-step procedure developed by Ballini and co-workers²⁹ (Scheme 1). First, treatment of **32** with hydrazine formed the hydrazinosulfone, which was converted directly to sulfones **33**–**39** with 2 equiv of the appropriate alkyl bromide or alkyl iodide and sodium acetate in EtOH at reflux. The reduction of lactams **33**–**39** with diborane yielded the desired 7-alkylsulfonyl-3-fluoromethyl-THIQs **23**–**29**.

Table 2. In Vitro Activities of 3-Fluoromethyl-7-sulfonyl-THIQs and 3-Fluoromethyl-7-(*N*-substituted Aminosulfonyl)-THIQs


compd	X	R	K_i (μM) \pm SEM ^a		selectivity α_2/hPNMT	ClogP ^c
			hPNMT	α_2^b		
18 ^d	NH	CH ₂ CH ₂ CF ₃	0.22 \pm 0.02	660 \pm 80	3000	1.88
19 ^e	NH	CH ₃	3.7 \pm 0.5 ^d	310 \pm 10	84	0.66
20 ^d	NH	CH ₂ CH ₃	1.4 \pm 0.1	550 \pm 60	390	1.01
21 ^d	NH	CH ₂ CH ₂ CH ₃	1.7 \pm 0.2	610 \pm 60	360	1.48
22 ^d	NH	CH ₂ CH ₂ OCH ₃	5.1 \pm 0.7	430 \pm 50	84	0.50
23	CH ₂	4-Cl-Ph	32 \pm 2	>1000 ^f	>31	3.09
24	CH ₂	CH ₂ CF ₃	1.3 \pm 0.1	>1000 ^f	>770	2.02
25	CH ₂	CH ₂ CH ₂ CF ₃	67 \pm 4	>1000 ^f	>15	2.27
26	CH ₂	CH ₃	14 \pm 1	1100 \pm 100	79	1.14
27	CH ₂	CH ₂ CH ₃	2.4 \pm 0.1	690 \pm 50	290	1.61
28	CH ₂	CH ₂ CH ₂ CH ₃	18 \pm 1	540 \pm 50	30	2.01
29	CH ₂	CH ₂ CH ₂ OCH ₃	72 \pm 7	1200 \pm 100	17	0.69
30	CH ₂	CF ₃	1.4 \pm 0.1	740 \pm 80	530	1.97
31 ^e	CH ₂	H	1.1 \pm 0.1	230 \pm 10	210	0.74

^a Standard error of the mean. ^b In vitro activities for the inhibition of [³H]clonidine binding to the α_2 -adrenoceptor. ^c Reference 37. ^d Reference 27. ^e Reference 23. ^f Could not be accurately determined due to precipitation at high assay concentrations.

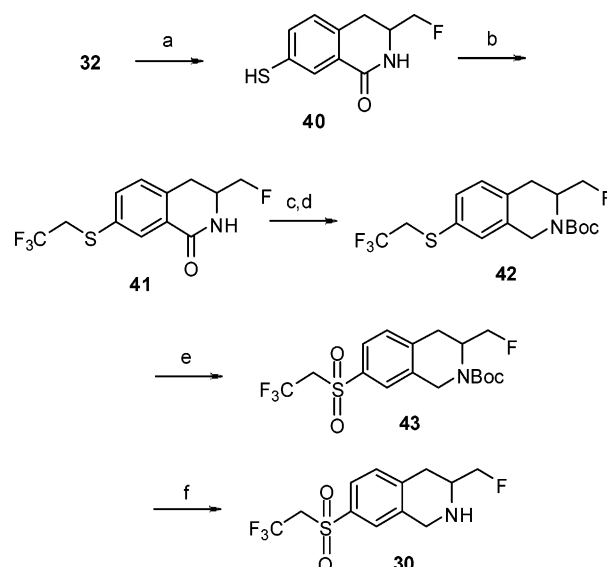
Scheme 1^a

^a Reagents and conditions: (a) NH₂NH₂, THF; then RBr or RI, NaOAc, EtOH; (b) BH₃·THF.

THIQ **30** (Table 2) could not be prepared according to the procedure described in Scheme 1 because the sulfone intermediate could not be synthesized from sulfonyl chloride **32**. An alternative route was developed and is described in Scheme 2. Sulfonyl chloride **32** was reduced to thiol **40** with tin sulfide and hydrochloric acid in acetic acid.³⁰ Based on a procedure for synthesizing fluoroalkyl aryl ethers from phenols,³¹ thiol **40** was converted to its potassium salt with potassium fluoride and then reacted with 1-iodo-2,2,2-trifluoroethane in DMSO in a sealed tube at 120 °C to afford sulfide **41**. The reduction of **41** with diborane followed by Boc protection of the resulting amine yielded **42**. Oxidation of the sulfide group of **42** with *m*-CPBA yielded **43**, which was deprotected with trifluoroacetic acid to afford THIQ **30**.

Biochemistry. In the current study, hPNMT with a C-terminal hexahistidine tag was expressed in *Escherichia coli*.^{27,32} The radiochemical assay conditions, previously reported for the bovine enzyme,³³ were modified to account for the high binding affinity of some inhibitors.^{27,34} Inhibition constants were determined using four concentrations of phenylethanolamine as the variable substrate and three concentrations of inhibitor.

α_2 -Adrenergic receptor binding assays were performed using cortex obtained from male Sprague Dawley rats.³⁵ [³H]Clonidine was used as the radioligand to define the specific binding and phentolamine was used to define the nonspecific binding.

Scheme 2^a

^a Reagents and conditions: (a) SnCl₂·2H₂O, HCl, AcOH; (b) KF, MeOH; then CF₃CH₂I, DMSO; (c) BH₃·THF; (d) Boc₂O, TEA, DMAP; (e) *m*-CPBA; (f) trifluoroacetic acid.

Clonidine was used as the ligand to define α_2 -adrenergic binding affinity to simplify the comparison with previous results.³⁶

Results and Discussion

The biochemical data for the 7-alkylsulfonyl-3-fluoromethyl-THIQs **23–31** is shown in Table 2, along with previously reported data for sulfonamides **18–22**, to determine the influence of the sulfonamide –NH– on PNMT inhibitory potency. Replacement of the sulfonamide –NH– with a methylene group resulted in compounds having higher ClogP values,³⁷ making them more likely to cross the BBB. However, a comparison of the hPNMT inhibitory potencies of sulfones **23–31** with sulfonamides **7, 14, 16**, and **18–22** clearly shows that the sulfonamide –NH– is playing an important role in the binding of these compounds, because all of the sulfonamides in Tables 1 and 2 are more potent than the corresponding sulfones.

This result was not expected, because analysis of the crystal structure of hPNMT cocrystallized with **7** indicated that the

Table 3. Crystallographic Data for hPNMT Co-Crystallized with (\pm)-**15** and **4**

hPNMT· 15 · 4 complex	
resolution	2.15 Å
space group	$P4_32_12$
Unit Cell	
<i>a</i> , <i>b</i>	94.3
<i>c</i>	188.9
α , β , γ	90
observations	366 364
unique reflections	47 217
resolution range (Å; top shell)	45.78–2.15 (2.23–2.15)
redundancy	7.76 (7.69)
<i>I</i> / σ <i>I</i>	16.7 (4.8)
completeness ^a (%)	99.9 (99.7)
rmerge ^b (%)	4.9 (40.2)
Refinement	
No. Reflections ($ F > 0$)	
total	47 132
(test set)	(4737)
rcryst ^c /rfree ^d (%)	20.0/24.2
(top shell)	(28.7/31.5)
No. non-hydrogen atoms	4636
protein nonhydrogen atoms	4232
ligand nonhydrogen atoms	98
waters	306
rmsd from Ideal Geometry	
bond length (Å)	0.009
bond angle (deg)	1.42
Coordinate Error	
ESD from Luzzati plot (Å)	0.26
ESD from C. V. Luzzati plot (Å)	0.32
Average B-Factor (Å ²)	
all	50.9
protein	50.6
ligand	44.5
water	57.1
Ramachandran Plot	
% in most favored region	93.3
% in disallowed region	0

^a Completeness indicates the number of measured independent reflections divided by the total number of theoretical independent reflections. ^b $R_{\text{merge}} = \sum |I_{\text{obs}} - I_{\text{av}}| / \sum I_{\text{av}}$, over all symmetry related observations. ^c $R_{\text{cryst}} = \sum |F_{\text{obs}} - F_{\text{calc}}| / \sum |F_{\text{obs}}|$, over all reflections. ^d R_{free} is calculated as for R_{cryst} from 10% of the data excluded from refinement. Values in parentheses are for the top shell of data.

sulfonamide $-\text{NH}_2-$ appears to form no favorable interactions with the enzyme (Figure 2). It was not until the acquisition of the X-ray crystal structure of hPNMT cocrystallized with **15** and **4** (hPNMT·**15**·**4**, Table 3, Figure 3) that these results could be interpreted.

There are significant differences between the X-ray crystal structure of hPNMT·**15**·**4** and the structure of hPNMT·**7**·**4** (Figure 2). One important difference is that the structure of hPNMT·**15**·**4** indicates the presence of a hydrogen bond between the sulfonamide $-\text{NH}-$ of **15** and the main chain carbonyl oxygen of Asn39. This interaction was not present in the crystal structure of hPNMT·**7**·**4** (Figure 2) and was overlooked in prior docking studies with 7-*N*-substituted-aminosulfonyl-THIQs (using the crystal structure of hPNMT·**7**·**4**).^{28,38,39} The results from the analysis of this new crystal structure and our new biochemical data strongly suggest that this interaction between Asn39 and the sulfonamide $-\text{NH}-$ is important, not only for the binding of **15**, but for the binding of the other 7-*N*-substituted-aminosulfonyl-THIQs.

Another major difference between these two crystal structures is that in hPNMT·**15**·**4** the side chain of Lys57 is shifted away from the sulfonamide of **15** to accommodate the 4-chlorophenyl

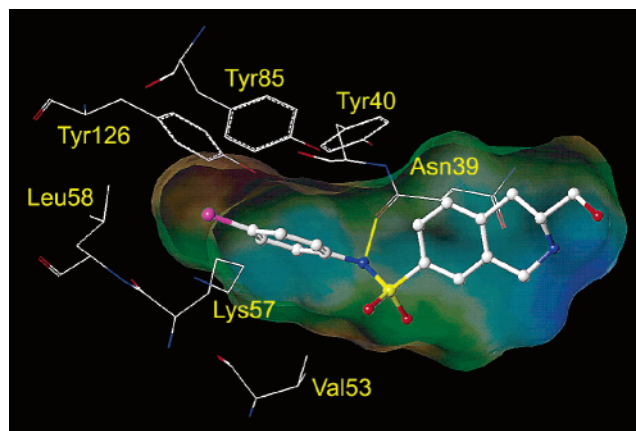


Figure 3. Active site of hPNMT cocrystallized with **15**. A Connolly (solvent accessible) surface exposing **15** is also shown. A lipophilic potential is mapped on the Connolly surface, whereby the areas shown in green are neutral, blue are hydrophilic, and brown are lipophilic. The sulfonamide oxygens of **15** are unable to form favorable interactions with the enzyme because the side chain of Lys57 is shifted away to accommodate the 4-chlorophenyl group of **15**. The hydrogen bond between the sulfonamide nitrogen of **15** and the main chain carbonyl oxygen of Asn39 (3.0 Å) is shown in yellow. Carbon is white, nitrogen is blue, oxygen is red, sulfur is yellow, and chlorine is magenta. Hydrogens are not shown for clarity.

group, and in hPNMT·**7**·**4**, the side chain of Lys57 forms hydrogen bonds with the sulfonamide oxygens of **7**.²² Also, the water-mediated hydrogen bond between one of the sulfonamide oxygens of **7** and Tyr126 and Arg44 is not observed, as this water molecule is displaced by the 4-chlorophenyl substituent of **15**.

Neither of the sulfonamide oxygens of **15** form hydrogen bonds with Lys57, nor does either of the sulfonamide oxygens participate in a water-mediated hydrogen bond, but the sulfonamide $-\text{NH}-$ gains a hydrogen bonding interaction, resulting in a net loss of two hydrogen bonds compared with **7** (and by extension as compared with **13**, the sulfonamide group of which is predicted to bind in the same manner as **7**). Because **15** and **13** are virtually equipotent at hPNMT, this net loss of two hydrogen bonds is apparently counterbalanced by additional hydrophobic interactions between the 4-chlorophenyl group of **15** and the five lipophilic residues (Tyr40, Val53, Leu58, Tyr85, and Tyr126), which are all within 3.8 Å of the 4-chlorophenyl group (Figure 3).

Docking studies (AutoDock 3.0)⁴⁰ were performed on sulfonamide **14** (Figure 4A) and sulfone **23** (Figure 4B) to compare the interactions of these two isosteric compounds with the active site of hPNMT. The docking results for both of these compounds indicate that they bind very much like **15**. The 4-chlorophenyl groups of **23** and **14** are predicted to make the same favorable hydrophobic interactions as **15**. The sulfonamide $-\text{NH}-$ of **14** and the α -methylene group of sulfone **23** occupy the same area in the active site as the sulfonamide $-\text{NH}-$ of **15**, but only the sulfonamide $-\text{NH}-$ of **14** is able to form a hydrogen bond with the main chain carbonyl oxygen of Asn39. We attribute most of the greater than 100-fold loss of hPNMT inhibitory potency of **23** versus **14** to the absence of this key interaction, but another factor could be contributing to this large decrease in potency. The sulfone group of **23** provides more degrees of conformational freedom than the corresponding sulfonamide group of **14** because the sulfonamide nitrogen is conjugated with the 4-chlorophenyl group and the sulfonamide sulfur.

For compounds having small 7-substituents, such as sulfones **24**, **26**, **27**, and **30** and sulfonamides **16**, **19**, and **20**,^{27,38} docking

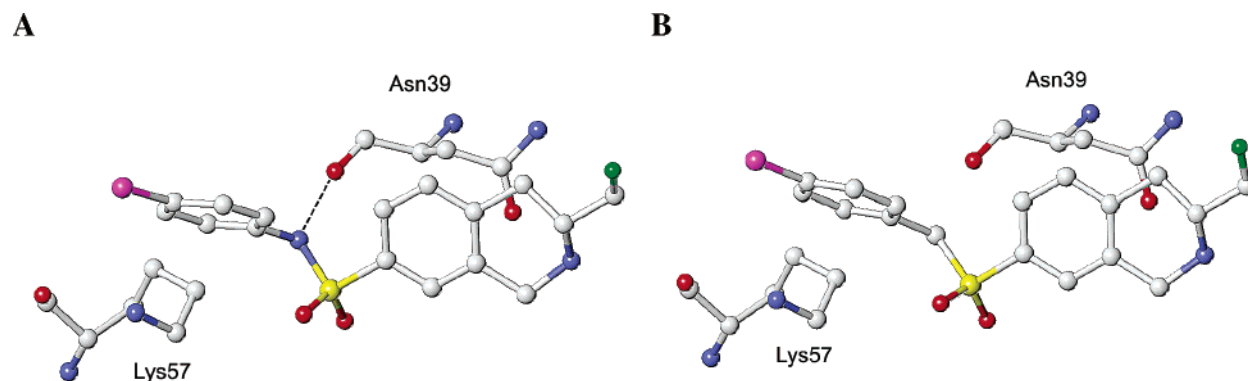


Figure 4. This figure shows a comparison of sulfonamide **14** and the corresponding isosteric sulfone **23** docked into the active site of hPNMT (modeled from the crystal structure of hPNMT in complex with **15**) and some of the key residues that could interact with **14** and **23**. Carbon is white, nitrogen is blue, oxygen is red, sulfur is yellow, fluorine is green, and chlorine is magenta. Hydrogens are not shown for clarity. (A) Similarly to **15** (Figure 3), the sulfonamide oxygens of **14** are unable to form favorable interactions with the enzyme because the side chain of Lys57 is shifted away to accommodate the 4-chlorophenyl group of **14**. The sulfonamide -NH- , however, is predicted to form a hydrogen bond with the main chain carbonyl oxygen of Asn39 (2.7 Å), as is observed with **15**. (B) Similarly to **14** and **15**, the sulfone oxygens of **23** are unable to form favorable interactions with the enzyme because the side chain of Lys57 is shifted away to accommodate the 4-chlorobenzyl group of **23**. In this case, there is no hydrogen bonding interaction with Asn39, as is observed for **15** in Figure 3 and predicted for **14**. This loss of a hydrogen bond in comparison to **14** is likely to be the molecular basis for the reduced PNMT inhibitory potency of **23** versus **14**.

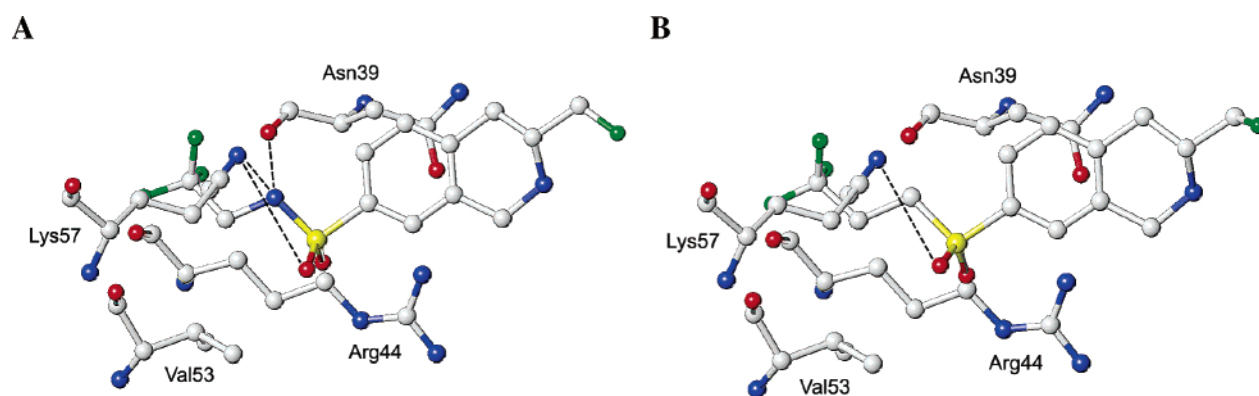


Figure 5. This figure shows a comparison of sulfonamide **16** and the corresponding isosteric sulfone **24** docked into the active site of hPNMT (modeled from the crystal structure of hPNMT in complex with **7**) and some of the key residues that could interact with **16** and **24**. Carbon is white, nitrogen is blue, oxygen is red, sulfur is yellow, and fluorine is green. Hydrogens are not shown for clarity. (A) The docking results with **16** indicate that the side chain of Lys57 is able to hydrogen bond to one of the sulfonamide oxygens (3.6 Å). These docking results also predict that the water molecule, which forms key interactions in the crystal structure of hPNMT in complex with **7** (Figure 2), is apparently displaced by the trifluoroethyl group of **16**. The sulfonamide nitrogen, however, is predicted to form a hydrogen bond with the main chain carbonyl oxygen of Asn39 (3.2 Å) and Lys57 (2.8 Å). (B) The docking results with **24** indicate that, similarly to **16**, the side chain of Lys57 is able to hydrogen bond to one of the sulfone oxygens (3.3 Å). These docking results also predict that the water molecule, which forms key interactions in the crystal structure of hPNMT in complex with **7**, is apparently displaced by the trifluoropropyl group of **24**. Note the absence of the hydrogen bonding interactions with Asn39 and Lys57 that are observed in Figure 5A. This loss of hydrogen bonds in comparison to **16** is likely to be the molecular basis for the reduced PNMT inhibitory potency of **24** versus **16**.

studies (using the crystal structure of hPNMT cocrystallized with **7**) indicate that the binding of these compounds does not require movement of the side chain of Lys57 away from the sulfonamide oxygens. These studies indicate that only one of the sulfonamide oxygens of **16** (Figure 5A) or one of the sulfone oxygens of **24** (Figure 5B) is able to form a hydrogen bond with Lys57. This differs from **7** (Figure 2, where both of the sulfonamide oxygens hydrogen bond with Lys57) and **15** (Figure 3, where neither of the sulfonamide oxygens hydrogen bond with Lys57). These studies also indicate that the water molecule that is predicted to form key interactions in the structure of hPNMT·**7**·**4** (Figure 2) is displaced by the trifluoroethyl group of **16** or the trifluoropropyl group of **24**. Similarly to **14** and **15**, the sulfonamide nitrogen of **16** is predicted to be within hydrogen bonding distance of the main chain carbonyl oxygen of Asn39. Unlike **14** and **15**, sulfonamide -NH- of **16** is predicted to be within hydrogen bonding distance of Lys57. Docking studies indicate that the α -methylene group of sulfone **24** occupies the same area in the active site as the sulfonamide -NH- of **16**,

but only the sulfonamide -NH- of **16** is able to form hydrogen bonds with Asn39 and Lys57. This is reflected in the 10-fold loss of hPNMT inhibitory potency of **24** versus **16**. Similar results were obtained in docking studies that compared sulfones **26** or **27** with sulfonamides **19** or **20** (data not shown).

A curious data trend was observed for sulfones **26**, **27**, and **31**. The ethyl sulfone (**26**) is less potent than the methyl sulfone (**31**) or the propyl sulfone (**27**). The same data trend is observed for the corresponding isosteric sulfonamides (**7**, **19**, and **20**).²⁷ This data trend can be explained with docking studies using the crystal structure of hPNMT·**7**·**4**. The methyl group of sulfone **31**²³ is predicted to occupy the same area in the active site as the sulfonamide $\text{-NH}_2\text{-}$ of **7** (Figure 2). Thus, similarly to **7**, both sulfone oxygens are able to interact with Lys57 through hydrogen bonds, and one of the sulfone oxygens is able to participate in a water-mediated hydrogen bond. Docking studies indicate that sulfones **26** (ethyl) and **27** (propyl) bind similarly to **24** (trifluoropropyl, Figure 4B). Only one of the sulfone oxygens is able to interact with hPNMT. According to docking

studies (data not shown), the propyl group of **27** is predicted to extend into the auxiliary binding pocket and make favorable hydrophobic interactions with Val53 and Arg44. These hydrophobic interactions apparently compensate for the loss of hydrogen bonding interactions of **27** (propyl) in comparison to **31** (methyl) because the hPNMT inhibitory potency of these compounds is quite similar. The ethyl group of sulfone **26**, however, is not predicted to extend into the binding pocket, which explains its decrease in PNMT inhibitory potency versus **27** (propyl). Docking studies (not shown) and data trends indicate that similarly to **27** (propyl), sulfone **30** (trifluoroethyl) is also able to make favorable hydrophobic interactions with the enzyme.

For compounds having larger 7-substituents, such as sulfones **25**, **28**, and **29** and sulfonamides²⁷ **18**, **21**, and **22**, docking studies indicate that Lys57 or other residues surrounding the binding pocket adjacent to the 7-position of THIQ must move to accommodate these larger groups. The reduction in hPNMT inhibitory potency of sulfones **25**, **28**, and **29** versus sulfones **24**, **27**, **30**, and **31**, which have smaller 7-substituents, is likely due to their inability to form hydrogen bonds with Lys57. The cocrystallization of one of these compounds is required to determine the exact nature of their binding. That being said, the data trends indicate that the sulfonamide $-NH-$ is required for optimal binding. We hypothesize that this is due to the ability of the sulfonamide $-NH-$ to form a hydrogen bond with Asn39 or Lys57.

In conclusion, the series of 3-fluoromethyl-7-sulfonyl-THIQs is more lipophilic but less potent than the corresponding sulfonamides. Sulfone **24** (hPNMT $K_i = 1.3 \mu\text{M}$) is the most potent compound in this series and is quite selective for PNMT versus the α_2 -adrenoceptor, but **24** is less potent than the corresponding sulfonamide, **16** (hPNMT $K_i = 0.13 \mu\text{M}$). This study has also identified a potential hydrogen bond acceptor within the hPNMT active site, the main chain carbonyl oxygen of Asn39, the importance of which is illustrated by comparing the potency of this series of sulfones to their corresponding sulfonamides. This discovery can now be applied toward the design of more potent inhibitors of PNMT.

Experimental Section

All reagents and solvents were of reagent grade or were purified by standard methods before use. Melting points were determined in open capillary tubes on a Thomas-Hoover melting point apparatus calibrated with known compounds. Proton (^1H NMR) and carbon (^{13}C NMR) nuclear magnetic resonance spectra were taken on a Bruker AM-500 spectrophotometer. High-resolution mass spectra (HRMS) were obtained on a Ribermag R 10-10 mass spectrophotometer. Flash chromatography was performed using silica gel 60 (230–400 mesh), supplied by Universal Adsorbents, Atlanta, Georgia.

Anhydrous methanol and ethanol were used unless stated otherwise and were prepared by distillation over magnesium. Other solvents were routinely distilled prior to use. Anhydrous tetrahydrofuran (THF) and diethyl ether (Et_2O) were distilled from sodium-benzophenone ketyl. Hexanes refers to the mixture of hexane isomers (bp 40–70 °C), and brine refers to a saturated solution of NaCl. All reactions that required anhydrous conditions were performed under a positive nitrogen or argon flow, and all glassware was either oven-dried or flame-dried before use. [*methyl*- ^3H]AdoMet and [^3H]clonidine were obtained from Perkin Elmer (Boston, MA).

Crystallography. His-tagged hPNMT was expressed, purified, and crystallized, as described previously.⁴¹ X-ray diffraction data were measured using a Rigaku FR-E copper rotating anode generator operating at 45 kV, 45 mA with Osmic Confocal Max-Flux optics (HiRes²) and an R-AXIS IV²⁺ imaging plate area detector. Data were processed using Crystal Clear (Rigaku Corpora-

tion, (c) 1997–2002), and phasing was carried out using CNS v1.1.⁴² The structure was solved by difference Fourier methods using the structure of hPNMT·**7-4** (PDB 1HNN)²² as the starting model. Model building was performed using O,⁴³ and the structure was refined using CNS v1.1.⁴² Topology and parameter files were generated using PRODRG⁴⁴ or XPLO2D.⁴⁵ The procedure used was to refine the structure of the protein first, then add waters, followed by addition of **4** and finally **15**. *R*-free analysis (10% of reflections) was used for cross-validation.⁴⁶ A racemic mixture of **15** was used in the crystallization experiment, but the *R*-enantiomer accounted for the density in the active site much better than the *S*-enantiomer. This result was expected because previous studies on 3-substituted-THIQs indicated that the *R*-enantiomer is preferred over the *S*-enantiomer in the hPNMT active site.^{38,47} Coordinates and structure factors for the crystal structure of hPNMT·**15-4** have been deposited as Protein Data Bank entry 2G8N.

Radiochemical Assay of PNMT Inhibitors. A typical assay mixture consisted of 25 μL of 0.5 M phosphate buffer (pH 8.0), 25 μL of 50 μM unlabeled AdoMet, 5 μL of [*methyl*- ^3H]AdoMet, containing approximately 3×10^5 dpm (specific activity approximately 15 Ci/mmol), 25 μL of substrate solution (phenylethanolamine), 25 μL of inhibitor solution, 25 μL of enzyme preparation (containing 30 ng hPNMT and 25 μg of bovine serum albumin), and sufficient water to achieve a final volume of 250 μL . After incubation for 30 min at 37 °C, the reaction mixture was quenched by the addition of 250 μL of 0.5 M borate buffer (pH 10.0) and was extracted with 2 mL of toluene/isoamyl alcohol (7:3). A 1 mL portion of the organic layer was removed, transferred to a scintillation vial, and diluted with cocktail for counting. The mode of inhibition was ascertained to be competitive in all cases reported in Tables 1 and 2 by examination of the correlation coefficients (r^2) for the fit routines, as calculated in the enzyme kinetics module (version 1.1) in SigmaPlot (version 7.0).³² While all K_i values reported were calculated using competitive kinetics, it should be noted that there was not always a great difference between the r^2 values for the competitive model versus the noncompetitive model. All assays were run in duplicate with three inhibitor concentrations over a 5-fold range. K_i values were determined by a hyperbolic fit of the data using the single substrate–single inhibitor routine in the enzyme kinetics module (version 1.1) in SigmaPlot (version 7.0). For inhibitors with apparent IC_{50} values less than 0.1 μM (as determined by a preliminary screen of the compounds to be assayed), the enzyme kinetics tight binding inhibition routine was used to calculate the K_i values.

α_2 -Adrenoceptor Radioligand Binding Assay. The radioligand receptor binding assay was performed according to the method of U'Prichard et al.³⁵ Male Sprague–Dawley rats were decapitated, and the cortexes were dissected out and homogenized in 20 volumes (w/v) of ice-cold 50 mM Tris/HCl buffer (pH 7.7 at 25 °C). Homogenates were centrifuged thrice for 10 min at 50 000 $\times g$ with resuspension of the pellet in fresh buffer between spins. The final pellet was homogenized in 200 volumes (w/v) of ice-cold 50 mM Tris/HCl buffer (pH 7.7 at 25 °C). Incubation tubes containing [^3H]clonidine (specific activity approximately 55 Ci/mmol, final concentration 2.0 nM) various concentrations of drugs and an aliquot of freshly resuspended tissue (800 μL) in a final volume of 1 mL were used. Tubes were incubated at 25 °C for 30 min, and the incubation was terminated by rapid filtration under vacuum through GF/B glass fiber filters. The filters were rinsed with three 5-mL washes of ice-cold 50 mM Tris buffer (pH 7.7 at 25 °C). The filters were counted in vials containing premixed scintillation cocktail. Nonspecific binding was defined as the concentration of bound ligand in the presence of 2 μM of phentolamine. All assays were run in quadruplicate with five inhibitor concentrations over a 16-fold range. IC_{50} values were determined by a log-probit analysis of the data, and K_i values were determined by the equation $K_i = \text{IC}_{50}/(1 + [\text{Clonidine}]/K_D)$, as all Hill coefficients were approximately equal to 1.

Molecular Modeling. Connolly surfaces were generated in SYBYL on a Silicon Graphics Octane workstation.⁴⁸ Docking of the various inhibitors into the PNMT active site was performed

using AutoDock 3.0.⁴⁰ The default settings for AutoDock 3.0 were used. The compound to be docked was initially overlaid with the cocrystallized ligand and minimized with the Tripos force field. The docking of inhibitors into the hPNMT active site was performed on the *R*-enantiomer, as a previous study on 3-substituted-THIQs indicated that the *R*-enantiomer is preferred over the *S*-enantiomer in the hPNMT active site.⁴⁷

General Procedure for the Preparation of Sulfones 33–39. Sulfonyl chloride **32** (between 0.35 and 0.80 mmol) was dissolved in THF (5–10 mL) and cooled to 0 °C. Hydrazine (3.5 equiv) was added dropwise to the solution, which was stirred overnight at ambient temperature. The solution was cooled to 0 °C, and the white precipitate (hydrazidosulfone) was collected by filtration. The precipitate was dissolved in EtOH (5 mL), and then NaOAc (10 equiv) and the requisite alkylbromide or alkyl iodide (5–10 equivalents) were added. The mixture was heated at reflux overnight. Water (50 mL) was added, and the solution was extracted with CH₂Cl₂ (3 × 40 mL). The combined organic extracts were washed with brine (40 mL) and dried over anhydrous Na₂SO₄. The solvent was removed under reduced pressure to yield the crude product, which was purified by flash chromatography.

(±)-3-Fluoromethyl-7-(4-chlorobenzylsulfonyl)-3,4-dihydroisoquinolin-1-2H-one (33). Sulfonyl chloride **32** (164 mg, 0.591 mmol) and 4-chlorobenzyl bromide (0.607 g, 2.96 mmol) were converted to **33** using the General Procedure for the Preparation of Sulfones. The crude product was purified by flash chromatography eluting with hexanes/acetone (2:1), followed by recrystallization from CHCl₃/hexanes, to yield **33** as a white crystals (69.1 mg, 0.188 mmol, 32%): mp 194–196 °C; ¹H NMR (500 MHz, CDCl₃) δ 8.47 (d, *J* = 1.9 Hz, 1H), 7.57–7.55 (m, 1H), 7.24 (d, *J* = 8.0 Hz, 1H), 7.19 (d, *J* = 8.5 Hz, 2H), 7.01 (d, *J* = 8.4 Hz, 2H), 6.12 (br, 1H), 4.49–4.31 (m, 2H, CH₂F), 4.24 (s, 2H), 4.08–4.01 (m, 1H), 3.09–2.92 (m, 2H); ¹³C NMR (500 MHz, CDCl₃) δ 163.4, 142.4, 137.8, 135.3, 132.3, 132.1, 129.4, 129.0, 128.6, 128.5, 126.2, 84.0 (d, *J* = 175 Hz), 61.8, 50.3 (d, *J* = 20.2 Hz), 29.1 (d, *J* = 6.4 Hz); HRMS (ESI⁺) *m/z* calcd for C₁₇H₁₆ClFNO₃S (MH⁺), 368.0523; found, 368.0536.

(±)-3-Fluoromethyl-7-(3,3,3-trifluoropropylsulfonyl)-3,4-dihydroisoquinolin-1-2H-one (34). Sulfonyl chloride **32** (204 mg, 0.735 mmol) and 1,1,1-trifluoro-3-iodopropane (0.90 mL, 7.22 mmol) were converted to **34** using the General Procedure for the Preparation of Sulfones. The crude product was purified by flash chromatography eluting with a gradient from hexanes/EtOAc (1:1) to hexanes/EtOAc (1:3) to yield **34** as a white solid (115 mg, 0.339 mmol, 46%): mp 231–233 °C; ¹H NMR (500 MHz, CDCl₃) δ 8.57 (d, *J* = 2.0 Hz, 1H), 7.98–7.96 (m, 1H), 7.44 (d, *J* = 8.0 Hz, 1H), 6.16 (br, 1H), 4.51–4.33 (m, 2H, CH₂F), 4.11–4.03 (m, 1H), 3.27–3.24 (m, 2H), 3.13–2.97 (m, 2H), 2.57–2.48 (m, 2H); ¹³C NMR (500 MHz, CDCl₃/DMSO-*d*₆ 4:1) δ 162.5, 142.9, 136.5, 130.3, 129.5, 128.7, 126.7, 124.6 (q, *J* = 277 Hz), 82.8 (d, *J* = 175 Hz), 49.1 (d, *J* = 21 Hz), 48.2 (q, *J* = 2.5 Hz), 28.4 (d, *J* = 4.9 Hz), 27.1 (q, *J* = 31 Hz); HRMS (ESI⁺) *m/z* calcd for C₁₃H₁₄F₄NO₃S (MH⁺), 340.0630; found, 340.0604.

(±)-3-Fluoromethyl-7-(4,4,4-trifluorobutylsulfonyl)-3,4-dihydroisoquinolin-1-2H-one (35). Sulfonyl chloride **32** (206 mg, 0.742 mmol) and 1,1,1-trifluoro-4-iodobutane (1.0 g, 2.83 mmol) were converted to **35** using the General Procedure for the Preparation of Sulfones. The crude product was purified by flash chromatography eluting with a gradient from hexanes/EtOAc (1:1) to hexanes/EtOAc (1:3) to yield **35** as a white solid (158 mg, 0.447 mmol, 60%): mp 118–120 °C; ¹H NMR (500 MHz, CDCl₃) δ 8.56 (d, *J* = 1.9 Hz, 1H), 7.97–7.95 (m, 1H), 7.42 (d, *J* = 8.0 Hz, 1H), 6.14 (br, 1H), 4.51–4.32 (m, 2H, CH₂F), 4.11–4.03 (m, 1H), 3.14–2.96 (m, 4H), 2.26–2.17 (m, 2H), 1.99–1.93 (m, 2H); ¹³C NMR (500 MHz, CDCl₃/DMSO-*d*₆ 4:1) δ 163.3, 143.0, 137.8, 131.0, 130.0, 129.1, 127.4, 126.3 (q, *J* = 277 Hz), 83.5 (d, *J* = 175 Hz), 54.2, 49.8 (d, *J* = 20.3 Hz), 31.9 (q, *J* = 29 Hz), 29.1 (d, *J* = 6.8 Hz), 15.7 (q, *J* = 3.4 Hz); HRMS (ESI⁺) *m/z* calcd for C₁₄H₁₆F₄NO₃S (MH⁺), 354.0787; found, 354.0770.

(±)-7-(3-Methoxypropylsulfonyl)-3-fluoromethyl-3,4-dihydroisoquinolin-1-2H-one (39). Sulfonyl chloride **32** (150 mg, 0.539

mmol) and 1-bromo-3-methoxypropane (0.41 g, 2.7 mmol) were converted to **39** using the General Procedure for the Preparation of Sulfones. The crude product was purified by flash chromatography eluting with hexanes/acetone (1:1), followed by recrystallization from EtOAc/hexanes, to yield **39** as a white solid (100 mg, 0.317 mmol, 59%): mp 109–111 °C; ¹H NMR (500 MHz, CDCl₃) δ 8.61 (d, *J* = 2.0 Hz, 1H), 8.03–8.01 (m, 1H), 7.47 (d, *J* = 8.0 Hz, 1H), 7.08 (br, 1H), 4.58–4.52 (m, 1H, CH₂F), 4.49–4.42 (m, 1H, CH₂F), 4.16–4.08 (m, 1H), 3.44 (t, *J* = 5.9 Hz, 2H), 3.29 (s, 3H), 3.26–3.23 (m, 2H), 3.21–3.05 (m, 2H), 2.02–1.97 (m, 2H); ¹³C NMR (500 MHz, CDCl₃) δ 163.0, 141.4, 137.9, 130.6, 128.5, 128.0, 127.8, 127.1, 82.8 (d, *J* = 175 Hz), 69.0, 57.6, 52.4, 49.3 (d, *J* = 20.4 Hz), 28.1 (d, *J* = 6.1 Hz), 22.2; HRMS (ESI⁺) *m/z* calcd for C₁₄H₁₉FNO₄S (MH⁺), 316.1019; found, 316.0999.

General Procedure for Lactam Reduction. Synthesis of 23–29. Lactams **33–39** (0.188–0.547 mmol) were dissolved in THF (10 mL), and 1 M BH₃·THF (10 equiv) was added. The solution was heated to reflux for 4 h and cooled to ambient temperature, and MeOH (15 mL) was added dropwise. The solvent was removed under reduced pressure, and to the remaining residue, a solution of MeOH (10 mL) and 6 N HCl (10 mL) was added. The mixture was heated to reflux for 3 h, and the MeOH was removed under reduced pressure. Water (25 mL) was added to the mixture, which was then made basic (pH ≈ 10) with 10% NaOH. The basic solution was extracted with CH₂Cl₂ (4 × 30 mL), and the combined organic extracts were dried over anhydrous Na₂SO₄. The solvent was removed under reduced pressure to yield the free amine, which was purified by flash chromatography, eluting with EtOAc. The free amine was dissolved in CHCl₃, and dry HCl(g) was bubbled through the solution to form the hydrochloride salt, which was recrystallized from EtOH/hexanes or MeOH/Et₂O to yield THIQs **24–29**. Compound **23** was recrystallized as the free base.

(±)-3-Fluoromethyl-7-(4-chlorobenzylsulfonyl)-1,2,3,4-tetrahydroisoquinoline (23). Compound **33** (69.1 mg, 0.188 mmol) was reduced to THIQ **23** according to the General Procedure for Lactam Reduction. The free base was recrystallized from EtOH/hexanes to yield **23** (58.4 mg, 0.165 mmol, 88%) as white crystals: mp 175–177 °C; ¹H NMR (500 MHz, CD₃OD) δ 7.19 (d, *J* = 8.1 Hz, 1H), 7.14 (s, 1H), 7.06 (d, *J* = 8.1 Hz, 1H), 7.03 (d, *J* = 8.3 Hz, 2H), 6.87 (d, *J* = 8.3 Hz, 2H), 4.37–4.13 (m, 2H, CH₂F), 3.81–3.73 (m, 4H), 3.03–2.94 (m, 1H), 2.65–2.94 (m, 2H); ¹³C NMR (500 MHz, CD₃OD) δ 140.3, 135.8, 135.2, 134.1, 132.0, 129.5, 127.9, 127.3, 126.0, 125.7, 84.9 (d, *J* = 169 Hz), 60.5, 52.4 (d, *J* = 19.2 Hz), 46.5, 28.8 (d, *J* = 7.3 Hz); HRMS (ESI⁺) *m/z* calcd for C₁₇H₁₈ClFNO₂S (MH⁺), 354.0731; found, 354.0726. Anal. (C₁₇H₁₇ClFNO₂S) C, H, N.

(±)-3-Fluoromethyl-7-(3,3,3-trifluoropropylsulfonyl)-1,2,3,4-tetrahydroisoquinoline Hydrochloride (24·HCl). Compound **34** (186 mg, 0.547 mmol) was reduced to THIQ **24** according to the General Procedure for Lactam Reduction. The hydrochloride salt was recrystallized from EtOH/hexanes to yield **24·HCl** (157 mg, 0.434 mmol, 79%) as white crystals: mp 238–240 °C; ¹H NMR (500 MHz, CD₃OD) δ 7.94–7.93 (m, 2H), 7.62 (d, *J* = 8.4 Hz, 1H), 4.97–4.69 (m, 2H, CH₂F), 4.65–4.58 (m, 2H), 4.02–3.95 (m, 1H), 3.55–3.52 (m, 2H), 3.35–3.21 (m, 2H), 2.67–2.58 (m, 2H); ¹³C NMR (500 MHz, CD₃OD) δ 137.9, 137.4, 130.4, 129.6, 127.4, 126.7, 125.8 (q, *J* = 275 Hz), 81.8 (d, *J* = 172 Hz), 53.0 (d, *J* = 19.0 Hz), 48.3 (q, *J* = 3.0 Hz), 44.4, 27.4 (q, *J* = 31.3 Hz), 26.2 (d, *J* = 5.9 Hz); HRMS (ESI⁺) *m/z* calcd for C₁₃H₁₆F₄NO₂S (MH⁺), 326.0838; found, 326.0818. Anal. (C₁₃H₁₆ClF₄NO₂S) C, H, N.

(±)-3-Fluoromethyl-7-(4,4,4-trifluorobutylsulfonyl)-1,2,3,4-tetrahydroisoquinoline Hydrochloride (25·HCl). Compound **35** (107 mg, 0.303 mmol) was reduced to THIQ **25** according to the General Procedure for Lactam Reduction. The hydrochloride salt was recrystallized from EtOH/hexanes to yield **25·HCl** (85.0 mg, 0.226 mmol, 75%) as white crystals: mp 225–227 °C; ¹H NMR (500 MHz, CD₃OD) δ 7.91–7.89 (m, 2H), 7.62 (d, *J* = 8.0 Hz, 1H), 4.97–4.68 (m, 2H, CH₂F), 4.65–4.59 (m, 2H), 4.02–3.95 (m, 1H), 3.38–3.20 (m, 4H), 2.41–2.32 (m, 2H), 1.95–1.89 (m, 2H); ¹³C NMR (500 MHz, CD₃OD) δ 137.9, 137.6, 130.3, 129.5,

127.3, 126.8 (q, $J = 276$ Hz), 126.4, 81.8 (d, $J = 172$ Hz), 53.6, 53.1 (d, $J = 18.6$ Hz), 31.3 (q, $J = 29$ Hz), 44.4, 26.2 (d, $J = 5.9$ Hz), 15.8 (q, $J = 3.5$ Hz); HRMS (ESI⁺) m/z calcd for C₁₄H₁₈F₄NO₂S (MH⁺), 340.0995; found, 340.0966. Anal. (C₁₄H₁₈ClF₄NO₂S) C, H, N.

(±)-**7-Ethylsulfonyl-3-fluoromethyl-1,2,3,4-tetrahydroisoquinoline Hydrochloride (26·HCl)**. Sulfonyl chloride **32** (150 mg, 0.539 mmol) and iodoethane (0.215 mL, 2.69 mmol) were converted to **36** using the General Procedure for the Preparation of Sulfones. The crude product was purified by flash chromatography eluting with hexanes/EtOAc (1:1) to yield **36** (100 mg, 0.369 mmol) as a white solid. Compound **36** was reduced to THIQ **26** according to the General Procedure for Lactam Reduction. The hydrochloride salt was recrystallized from MeOH/Et₂O to yield **26·HCl** (59.4 mg, 0.202 mmol, 37%, 2 steps) as white crystals: mp 245–247 °C; ¹H NMR (500 MHz, DMSO-*d*₆) δ 7.91 (s, 1H), 7.85–7.83 (m, 1H), 7.61 (d, $J = 8.2$ Hz, 1H), 5.01–4.89 (m, 1H, CH₂F), 4.86–4.74 (m, 1H, CH₂F), 4.58–4.50 (m, 2H), 4.03–3.94 (m, 1H), 3.35 (q, $J = 7.3$ Hz, 2H), 3.26–3.11 (m, 2H), 1.16 (t, $J = 7.3$ Hz, 3H); ¹³C NMR (500 MHz, DMSO-*d*₆) δ 137.5, 136.8, 130.1, 130.0, 126.6, 126.3, 82.1 (d, $J = 169$ Hz), 51.8 (d, $J = 19$ Hz), 49.1, 43.8, 26.1 (d, $J = 6.2$ Hz), 7.1; HRMS (FAB⁺) m/z calcd for C₁₂H₁₇FNO₂S (MH⁺), 258.0964; found, 258.0955. Anal. (C₁₂H₁₇ClFNO₂S) C, H, N.

(±)-**3-Fluoromethyl-7-propylsulfonyl-1,2,3,4-tetrahydroisoquinoline Hydrochloride (27·HCl)**. Sulfonyl chloride **32** (100 mg, 0.360 mmol) and iodopropane (0.18 mL, 1.8 mmol) were converted to **37** using the General Procedure for the Preparation of Sulfones. The crude product was purified by flash chromatography eluting with hexanes/EtOAc (1:2) to yield **37** (65.0 mg, 0.228 mmol) as a white solid. Compound **37** was reduced to THIQ **27** according to the General Procedure for Lactam Reduction. The hydrochloride salt was recrystallized from MeOH/Et₂O to yield **27·HCl** (36 mg, 0.12 mmol, 33%, 2 steps) as white crystals: mp 230–232 °C; ¹H NMR (500 MHz, DMSO-*d*₆) δ 7.85 (d, $J = 1.8$ Hz, 1H), 7.79–7.77 (m, 1H), 7.55 (d, $J = 8.2$ Hz, 1H), 4.95–4.83 (m, 1H, CH₂F), 4.80–4.68 (m, 1H, CH₂F), 4.52–4.44 (m, 2H), 3.97–3.88 (m, 1H), 3.29–3.26 (m, 2H), 3.20–3.05 (m, 2H), 1.59–1.51 (m, 2H), 0.92 (t, $J = 7.4$ Hz, 3H); ¹³C NMR (500 MHz, DMSO-*d*₆) δ 137.5, 137.4, 130.1, 130.0, 126.4, 126.2, 82.1 (d, $J = 169$ Hz), 56.1, 51.8 (d, $J = 19$ Hz), 43.8, 26.1 (d, $J = 6.1$ Hz), 16.2, 12.5; HRMS (FAB⁺) m/z calcd for C₁₃H₁₉FNO₂S (MH⁺), 272.1121; found, 272.1113. Anal. (C₁₃H₁₉ClFNO₂S) C, H, N.

(±)-**7-Butylsulfonyl-3-fluoromethyl-1,2,3,4-tetrahydroisoquinoline Hydrochloride (28·HCl)**. Sulfonyl chloride **32** (150 mg, 0.539 mmol) and iodobutane (0.31 mL, 2.7 mmol) were converted to **38** using the General Procedure for the Preparation of Sulfones. The crude product was purified by flash chromatography eluting with hexanes/EtOAc (1:2) to yield **38** (140 mg, 0.468 mmol) as a white solid. Compound **38** was reduced to THIQ **28** according to the General Procedure for Lactam Reduction. The hydrochloride salt was recrystallized from MeOH/Et₂O to yield **28·HCl** (106 mg, 0.329 mmol, 61%) as white crystals: mp 175–177 °C; ¹H NMR (500 MHz, DMSO-*d*₆) δ 7.86 (d, $J = 1.8$ Hz, 1H), 7.80–7.78 (m, 1H), 7.55 (d, $J = 8.2$ Hz, 1H), 4.95–4.83 (m, 1H, CH₂F), 4.80–4.68 (m, 1H, CH₂F), 4.52–4.45 (m, 2H), 3.97–3.88 (m, 1H), 3.31–3.28 (m, 2H), 3.21–3.05 (m, 2H), 1.53–1.47 (m, 2H), 1.37–1.30 (m, 2H), 0.83 (t, $J = 7.3$ Hz, 3H); ¹³C NMR (500 MHz, DMSO-*d*₆) δ 137.4, 137.4, 130.0, 130.0, 126.4, 126.2, 82.1 (d, $J = 169$ Hz), 54.2, 51.8 (d, $J = 19$ Hz), 43.8, 26.1 (d, $J = 6.3$ Hz), 24.3, 20.7, 13.4; HRMS (FAB⁺) m/z calcd for C₁₄H₂₁FNO₂S (MH⁺), 286.1277; found, 286.1259. Anal. (C₁₄H₂₁ClFNO₂S) C, H, N.

(±)-**7-(3-Methoxypropylsulfonyl)-3-fluoromethyl-1,2,3,4-tetrahydroisoquinoline Hydrochloride (29·HCl)**. Compound **39** (100 mg, 0.317 mmol) was reduced to THIQ **29** according to the General Procedure for Lactam Reduction. The hydrochloride salt was recrystallized from MeOH/Et₂O to yield **29·HCl** (52.0 mg, 0.154 mmol, 49%) as white crystals: mp 136–138 °C; ¹H NMR (500 MHz, CD₃OD) δ 7.89–7.87 (m, 2H), 7.60 (d, $J = 8.0$ Hz, 1H), 4.97–4.85 (m, 1H, CH₂F), 4.81–4.69 (m, 1H, CH₂F), 4.65–4.58 (m, 2H), 4.04–3.96 (m, 1H), 4.04–3.96 (t, $J = 6.0$ Hz, 2H), 3.31–

3.22 (m, 4H), 3.29 (s, 3H), 1.94–1.89 (m, 2H); ¹³C NMR (500 MHz, CD₃OD) δ 138.2, 137.3, 130.2, 129.3, 127.2, 126.4, 81.8 (d, $J = 172$ Hz), 69.6, 57.4, 53.1 (d, $J = 19$ Hz), 52.5, 44.4, 26.2 (d, $J = 5.9$ Hz), 22.9; HRMS (ESI⁺) m/z calcd for C₁₄H₂₁FNO₃S (MH⁺), 302.1226; found, 322.1205. Anal. (C₁₄H₂₁ClFNO₃S) C, H, N.

(±)-**3-Fluoromethyl-7-mercapto-3,4-dihydroisoquinolin-1-2H-one (40)**. Sulfonyl chloride **32** (700 mg, 2.6 mmol) was dissolved in glacial acetic acid (25 mL) and heated to 75 °C. A slurry of SnCl₂·2H₂O (4.0 g, 10.4 mmol) and HCl (3.5 mL) was added slowly to the solution of **32**. The reaction was allowed to cool to 25 °C and stirred for 1.5 h. 1 N HCl (100 mL) and brine (75 mL) were added, and the solution was extracted with CHCl₃ (5 × 75 mL). The combined organic extracts were washed with brine (50 mL) and dried over anhydrous Na₂SO₄. The solvent was removed under reduced pressure, and the crude product was purified by flash chromatography eluting with EtOAc to yield **40** (530 mg, 99%) as a yellow solid: ¹H NMR (500 MHz, CDCl₃) δ 8.20 (d, $J = 1.9$ Hz, 1H), 7.67–7.65 (m, 1H), 7.21 (d, $J = 8.0$ Hz, 1H), 6.15 (br, 1H), 4.55–4.48 (m, 1H, CH₂F), 4.44–4.36 (m, 1H, CH₂F), 4.11–4.01 (m, 1H), 3.56 (s, 1H, SH), 3.05–2.88 (m, 2H); HRMS (ESI⁺) m/z calcd for C₁₀H₁₁FNOS (MH⁺), 212.0545; found, 212.0523.

(±)-**3-Fluoromethyl-7-(2,2,2-trifluoroethylthio)-3,4-dihydroisoquinolin-1-2H-one (41)**. Potassium fluoride (0.120 g, 2.06 mmol) was added to a solution of **40** (435 mg, 2.06 mmol) in MeOH (10 mL) and then stirred for 20 min at 60 °C. The solvent was removed under reduced pressure, and the remaining solid was rinsed with Et₂O (3 × 10 mL). This solid (potassium salt of **40**) and 1-iodo-2,2,2-trifluoroethane (1.02 mL, 10.3 mmol) were dissolved in DMSO, transferred to a sealed tube, and heated to 120 °C with stirring for 16 h. The solution was cooled to 0 °C and ice water (50 mL) was added. This aqueous solution was extracted with CH₂-Cl₂ (4 × 50 mL), and the combined organic extracts were washed with brine (50 mL) and dried over anhydrous Na₂SO₄. The solvent was removed under reduced pressure to yield the crude product as a white solid, which was purified by flash chromatography eluting with EtOAc/hexanes (1:1) to yield **41** (413 mg, 1.41 mmol, 68%) as a white solid: mp 121–123 °C; ¹H NMR (500 MHz, CDCl₃) δ 8.23 (d, $J = 2.1$ Hz, 1H), 7.62–7.60 (m, 1H), 7.22 (d, $J = 7.9$ Hz, 1H), 6.15 (br, 1H), 4.57–4.38 (m, 2H, CH₂F), 4.13–4.04 (m, 1H), 3.50 (q, $J = 9.6$ Hz, 2H), 3.07–2.91 (m, 2H); ¹³C NMR (500 MHz, CDCl₃) δ 163.7, 135.1, 134.7, 132.2, 129.8, 127.9, 127.6, 124.1 (q, $J = 277$ Hz), 82.9 (d, $J = 175$ Hz), 49.4 (d, $J = 20$ Hz), 36.7 (q, $J = 33$ Hz), 27.4 (d, $J = 6.4$ Hz); HRMS (FAB⁺) m/z calcd for C₁₂H₁₂F₄NOS (MH⁺), 294.0576; found, 294.0556.

(±)-**2-(tert-Butoxycarbonyl)-3-fluoromethyl-7-(2,2,2-trifluoroethylthio)-1,2,3,4-tetrahydroisoquinoline (42)**. Lactam **41** (200 mg, 0.682 mmol) was dissolved in THF (10 mL), and 1 M BH₃·THF (3.1 mL, 3.1 mmol) was added. The solution was heated to reflux for 4 h and cooled to ambient temperature, and MeOH (15 mL) was added dropwise. The solvent was removed under reduced pressure, and to the remaining residue, a solution of MeOH (10 mL) and 6 N HCl (10 mL) was added. The mixture was heated to reflux for 3 h, and the MeOH was removed under reduced pressure. Water (25 mL) was added to the mixture, which was then made basic (pH ≈ 10) with 10% NaOH. The basic solution was extracted with CH₂Cl₂ (4 × 30 mL), and the combined organic extracts were dried over anhydrous Na₂SO₄. The solvent was removed under reduced pressure to yield the free amine, which was purified by flash chromatography eluting with CHCl₃/MeOH (3:1) to yield the THIQ intermediate as a yellow oil (160 mg), which was slightly impure according to ¹H NMR. This crude product was dissolved in CHCl₃ (10 mL), and DMAP (70 mg, 0.573 mmol) and TEA (0.077 mL, 0.573 mmol) were added. The solution was cooled to 0 °C and Boc₂O (0.264 mL, 1.15 mmol) was added dropwise. The solution was warmed to room temperature and stirred for 16 h. 1 M HCl (150 mL) was added to the reaction mixture, which was then extracted with CH₂Cl₂ (3 × 50 mL). The organic extracts were combined, washed with saturated NaHCO₃ (75 mL) and brine (75 mL), and dried over anhydrous Na₂SO₄. The solvent was removed under reduced pressure, and the residue was purified by flash

chromatography eluting with EtOAc/hexanes (1:5) to yield **42** as a white solid (80 mg, 0.21 mmol, 31%, 2 steps): $^1\text{H NMR}$ (500 MHz, CDCl_3) δ 7.28–7.26 (m, 1H), 7.21 (s, 1H), 7.08 (d, $J = 7.9$ Hz, 1H), 4.67–3.96 (m, 5H with major and minor rot.), 3.35 (q, $J = 9.7$ Hz, 2H), 2.99–2.80 (m, 2H), 1.43 (s, 9H); $^{13}\text{C NMR}$ (500 MHz, CDCl_3) δ 154.9, 134.6, 132.9, 131.7, 130.8, 129.9, 129.6, 125.3 (q, $J = 277$ Hz), 82.0 (d, $J = 174$ Hz), 80.7, 49.7 (minor rot.), 48.5 (major rot.), 43.9 (major rot.), 43.2 (minor rot.), 38.3 (q, $J = 32.6$ Hz), 29.0, 28.4; HRMS (ESI⁺) m/z calcd for $\text{C}_{17}\text{H}_{22}\text{F}_4\text{NO}_2\text{S}$ (MH⁺), 380.1308; found, 380.1301.

(±)-2-(*tert*-Butoxycarbonyl)-3-fluoromethyl-7-(2,2,2-trifluoroethylsulfonyl)-1,2,3,4-tetrahydroisoquinoline (**43**). Compound **42** (100 mg, 0.264 mmol) was dissolved in CH_2Cl_2 (10 mL) and *m*-CPBA (228 mg, 1.32 mmol) was added. The solution was stirred for 2 h at room temperature. NaHSO_3 (50 mL, 20% w/v) was then added, and the solution was extracted with CH_2Cl_2 (3 × 50 mL). The organic layer was washed with saturated NaHCO_3 (75 mL) and brine (75 mL) and dried over anhydrous Na_2SO_4 . The solvent was removed under reduced pressure, and the crude product was purified by flash chromatography eluting with acetone/hexanes (1:7) to yield **43** as a white solid (89.0 mg, 0.216 mmol, 82%): $^1\text{H NMR}$ (500 MHz, CDCl_3) δ 7.83 (d, $J = 8.0$ Hz, 1H), 7.77 (s, 1H), 7.46 (d, $J = 8.0$ Hz, 1H), 4.67–3.96 (m, 5H with major and minor rot.), 3.93 (q, $J = 9.0$ Hz, 2H), 3.21–3.05 (m, 2H), 1.53 (s, 9H); $^{13}\text{C NMR}$ (500 MHz, CDCl_3) δ 154.6, 140.7, 136.6, 135.2, 130.0, 126.9, 126.2, 121.0 (q, $J = 278$ Hz), 82.3 (d, $J = 166$ Hz), 81.0, 58.4 (q, $J = 31.3$ Hz), 49.3 (minor rot.), 48.1 (major rot.), 43.9 (major rot.), 43.1 (minor rot.), 29.6, 28.3; HRMS (FAB⁺) m/z calcd for $\text{C}_{17}\text{H}_{22}\text{F}_4\text{NO}_4\text{S}$ (MH⁺), 412.1206; found, 412.1197.

(±)-3-Fluoromethyl-7-(2,2,2-trifluoroethylsulfonyl)-1,2,3,4-tetrahydroisoquinoline Hydrochloride (**30**·HCl). Compound **43** (90 mg, 0.219 mmol) was dissolved in CH_2Cl_2 (6 mL) and trifluoroacetic acid (2 mL). The mixture was stirred at room temperature for 1 h. NaOH (100 mL, 5% w/v) was added, and the solution was extracted with CH_2Cl_2 (3 × 75 mL). The combined organic extracts were washed with brine (50 mL) and dried over anhydrous Na_2SO_4 . The solvent was removed under reduced pressure to yield a clear oil, which was purified by flash chromatography eluting with EtOAc/hexanes (4:1). The free amine was dissolved in CHCl_3 , and dry $\text{HCl}_{(\text{g})}$ was bubbled through the solution to form the hydrochloride salt, which was recrystallized from EtOH/hexanes to yield **30**·HCl (85 mg, 0.226 mmol, 75%) as white crystals: mp 229–231 °C; $^1\text{H NMR}$ (500 MHz, CD_3OD) δ 7.96–7.94 (m, 2H), 7.62 (d, $J = 7.9$ Hz, 1H), 4.97–4.85 (m, 1H, CH_2F), 4.81–4.69 (m, 1H, CH_2F), 4.66–4.58 (m, 2H), 4.54 (q, $J = 9.5$ Hz, 2H), 4.03–3.95 (m, 1H), 3.35–3.21 (m, 2H); $^{13}\text{C NMR}$ (500 MHz, CD_3OD) δ 138.2, 138.2, 130.3, 129.4, 127.6, 126.8, 121.8 (q, $J = 277$ Hz), 81.8 (d, $J = 171$ Hz), 56.6 (q, $J = 31.0$ Hz), 53.0 (d, $J = 19$ Hz), 44.4, 26.2 (d, $J = 5.8$ Hz); HRMS (FAB⁺) m/z calcd for $\text{C}_{12}\text{H}_{14}\text{F}_4\text{NO}_2\text{S}$ (MH⁺), 312.0681; found, 312.0664. Anal. ($\text{C}_{12}\text{H}_{14}\text{ClF}_4\text{NO}_2\text{S}$) C, H, N.

Acknowledgment. This research was supported by National Institutes of Health (NIH) Grant HL 34193 and Australian Research Council (ARC) Grant DP0345019. The funding for M.R.S. was also supported by NIH Predoctoral Training Grant GM 07775 and the American Foundation for Pharmaceutical Education. The funding of R.C.R. was also supported by the Madison and Lila Self-Graduate Fellowship and the Pfizer Summer Undergraduate Research Fellowship. We thank David VanderVelde and Sarah Neuenswander of the University of Kansas Nuclear Magnetic Resonance Laboratory for their assistance. The 500 MHz NMR spectrometer was partially funded by National Science Foundation Grant CHE-9977422. We thank Gerald Lushington of the University of Kansas Molecular Graphics and Modeling Laboratory and Todd Williams of the University of Kansas Mass Spectrometry Laboratory for their assistance.

Supporting Information Available: All elemental analyses (C, H, N) for assayed compounds are included. This material is available free of charge via the Internet at <http://pubs.acs.org>.

References

- (1) The contents of this paper were taken in large part from the Ph.D. dissertation (University of Kansas, 2006) of Mitchell R. Seim.
- (2) Vogt, M. The Concentration of Sympathin in Different Parts of the Central Nervous System Under Normal Conditions and After the Administration of Drugs. *J. Physiol. (London)* **1954**, *123*, 451–81.
- (3) Gunne, L. M. Relative Adrenaline Content in Brain Tissue. *Acta Biochim. Pol.* **1962**, *56*, 324–333.
- (4) Axelrod, J. Purification and Properties of Phenylethanolamine-*N*-methyltransferase. *J. Biol. Chem.* **1962**, *237*, 1657–1660.
- (5) Fuller, R. W. *Epinephrine in the Central Nervous System*; Oxford University Press: New York, 1988; pp 366–369.
- (6) Ruggiero, D. A.; Cravo, S. L.; Golanov, E.; Gomez, R.; Anwar, M.; Reis, D. J. Adrenergic and Non-Adrenergic Spinal Projections of a Cardiovascular-Active Pressor Area of Medulla Oblongata: Quantitative Topographic Analysis. *Brain Res.* **1994**, *663*, 107–120.
- (7) Crowley, W. R.; Terry, L. C. Effects of an Epinephrine Synthesis Inhibitor, SKF64139, on the Secretion of Luteinizing Hormone in Ovariectomized Female Rats. *Brain Res.* **1981**, *204*, 231–235.
- (8) Masaharu, K.; Atobe, M.; Nakagawara, M.; Kariya, T. Effect of a Phenylethanolamine *N*-Methyltransferase Inhibitor, 2,3-Dichloromethylbenzylamine, on the Alpha-2-adrenoceptor Function in the Hypothalamus in Rats. *Neuropsychobiology* **1996**, *33*, 132–137.
- (9) Burke, W. J.; Galvin, N. J.; Chung, H. D.; Stoff, S. A.; Gillespie, K. N.; Cataldo, A. M.; Nixon, R. A. Degenerative Changes in Epinephrine Tonic Vasomotor Neurons in Alzheimer's Disease. *Brain Res.* **1994**, *661*, 35–42.
- (10) Burke, W. J.; Chung, H. D.; Marshall, G. L.; Gillespie, K. N.; Joh, T. H. Evidence for Decreased Transport of PNMT Protein in Advanced Alzheimer's Disease. *J. Am. Geriatr. Soc.* **1990**, *38*, 1275–1282.
- (11) Burke, W. J.; Chung, H. D.; Strong, R.; Mattammal, M. B.; Marshall, G. L.; Nakra, R.; Grossberg, G. T.; Haring, J. H.; Joh, T. H. Mechanism of Degeneration of Epinephrine Neurons in Alzheimer's Disease. In *Central Nervous System Disorders of Aging: Clinical Intervention and Research*; Strong, R., Ed.; Raven Press: New York, 1988; pp 41–70.
- (12) Pendleton, R. G.; Kaiser, C.; Gessner, G. Studies on Adrenal Phenylethanolamine *N*-Methyltransferase (PNMT) with SK&F 64139, a Selective Inhibitor. *J. Pharmacol. Exp. Ther.* **1976**, *197*, 623–632.
- (13) Goldstein, M.; Kinguasa, K.; Hieble, J. P.; Pendleton, R. G. Lowering of Blood Pressure in Hypertensive Rats by SK&F 64139 and SK&F 72223. *Life Sci.* **1982**, *30*, 1951–1957.
- (14) Toomey, R. E.; Hornig, J. S.; Hemrick-Luecke, S. K.; Fuller, R. W. α_2 -Adrenoceptor Affinity of Some Inhibitors of Norepinephrine *N*-Methyltransferase. *Life Sci.* **1981**, *29*, 2467–2472.
- (15) Goldstein, M.; Saito, M.; Lew, J. Y.; Hieble, J. P.; Pendleton, R. G. The Blockade of α_2 -Adrenoceptors by the PNMT Inhibitor SK&F 64139. *Eur. J. Pharmacol.* **1980**, *67*, 305–308.
- (16) Drew, G. M. α_2 -Adrenoceptor-Blocking Action of the Phenylethanolamine-*N*-methyltransferase Inhibitor SK&F 64139. *J. Pharm. Pharmacol.* **1981**, *33*, 187–188.
- (17) Pendleton, R. G.; Hieble, J. P. Studies on the Adrenergic Receptor Specificity of Inhibitors of Phenylethanolamine *N*-Methyltransferase. *Res. Commun. Chem. Pathol. Pharmacol.* **1981**, *34*, 399–408.
- (18) Pendleton, R. G.; Gessner, G.; Weiner, G.; Jenkins, B.; Sawyer, J.; Bondinell, W.; Intoccia, A. Studies on SK&F 29661, an Organ-Specific Inhibitor of Phenylethanolamine *N*-Methyltransferase. *J. Pharmacol. Exp. Ther.* **1979**, *208*, 24–30.
- (19) Blank, B.; Krog, A. J.; Weiner, G.; Pendleton, R. G. Inhibitors of Phenylethanolamine *N*-Methyltransferase and Epinephrine Biosynthesis. 2. 1,2,3,4-Tetrahydroisoquinoline-7-sulfonanilides. *J. Med. Chem.* **1980**, *23*, 837–840.
- (20) Grunewald, G. L.; Dahanukar, V. H.; Caldwell, T. M.; Criscione, K. R. Examination of the Role of the Acidic Hydrogen in Imparting Selectivity of 7-(Aminosulfonyl)-1,2,3,4-tetrahydroisoquinoline (SK&F 29661) Toward Inhibition of Phenylethanolamine-*N*-Methyltransferase vs the α_2 -Adrenoceptor. *J. Med. Chem.* **1997**, *40*, 3997–4005.
- (21) Grunewald, G. L.; Dahanukar, V. H.; Jalluri, R. K.; Criscione, K. R. Synthesis, Biochemical Evaluation, and Classical and Three-Dimensional Quantitative Structure–Activity Relationship Studies of 7-Substituted-1,2,3,4-tetrahydroisoquinolines and Their Relative Affinities Toward Phenylethanolamine *N*-Methyltransferase and the α_2 -Adrenoceptor. *J. Med. Chem.* **1999**, *42*, 118–134.

- (22) Martin, J. L.; Begun, J.; McLeish, M. J.; Caine, J. M.; Grunewald, G. L. Getting the Adrenaline Going: Crystal Structure of the Adrenaline-Synthesizing Enzyme PNMT. *Structure* **2001**, *9*, 977–985.
- (23) Grunewald, G. L.; Caldwell, T. M.; Li, Q. F.; Slavica, M.; Criscione, K. R.; Borchardt, R. T.; Wang, W. Synthesis and Biochemical Evaluation of 3-Fluoromethyl-1,2,3,4-tetrahydroisoquinolines as Selective Inhibitors of Phenylethanolamine *N*-Methyltransferase versus the α_2 -Adrenoceptor. *J. Med. Chem.* **1999**, *42*, 3588–3601.
- (24) Grunewald, G. L.; Dahanukar, V. H.; Teoh, B.; Criscione, K. R. 3,7-Disubstituted-1,2,3,4-tetrahydroisoquinolines Display Remarkable Potency and Selectivity as Inhibitors of Phenylethanolamine *N*-Methyltransferase versus the α_2 -Adrenoceptor. *J. Med. Chem.* **1999**, *42*, 1982–1990.
- (25) Takakura, Y.; Audus, K. L.; Borchardt, R. T. Blood-Brain Barrier: Transport Studies in Isolated Brain Capillaries and in Cultured Brain Endothelial Cells. *Adv. Pharmacol.* **1991**, *22*, 137–165.
- (26) Audus, K. L.; Borchardt, R. T. Characterization of an In Vitro Blood-Brain Barrier Model System for Studying Drug Transport and Metabolism. *Pharm. Res.* **1986**, *3*, 81–87.
- (27) Romero, F. A.; Vodonick, S. M.; Criscione, K. R.; McLeish, M. J.; Grunewald, G. L. Inhibitors of Phenylethanolamine *N*-Methyltransferase that are Predicted to Penetrate the Blood-Brain Barrier: Design, Synthesis, and Evaluation of 3-Fluoromethyl-7-(*N*-substituted aminosulfonyl)-1,2,3,4-tetrahydroisoquinolines that Possess Low Affinity Toward the α_2 -Adrenoceptor. *J. Med. Chem.* **2004**, *47*, 4483–4493.
- (28) Grunewald, G. L.; Romero, F. A.; Criscione, K. R. 3-Hydroxymethyl-7-(*N*-substituted aminosulfonyl)-1,2,3,4-tetrahydroisoquinoline Inhibitors of Phenylethanolamine *N*-Methyltransferase that Display Remarkable Potency and Selectivity. *J. Med. Chem.* **2005**, *48*, 134–140.
- (29) Ballini, R.; Marcantoni, E.; Petrini, M. A. New General Synthesis of Sulfones from Alkyl or Aryl Halides and *p*-Toluenesulfonyl Hydrazide. *Tetrahedron* **1989**, *45*, 6791–6798.
- (30) Bondinell, W. E.; Pendleton, R. G. 7- and/or 8-Sulfur Substituted 1,2,3,4-Tetrahydroisoquinoline Compounds. U.S. Patent 4,228,170, Oct. 14, 1980.
- (31) Kamal, A.; Pratap, T. B.; Ramana, K. V.; Ramana, A. V.; Babu, A. H. Facile and Efficient Synthesis of Fluoroalkyl Aryl Ethers. *Tetrahedron Lett.* **2002**, *43*, 7353–7355.
- (32) Caine, J. M.; Macreadie, I. G.; Grunewald, G. L.; McLeish, M. J. Recombinant Human Phenylethanolamine *N*-Methyltransferase: Overproduction in *Escheria coli*, Purification and Characterization. *Protein Expression Purif.* **1996**, *8*, 160–166.
- (33) Grunewald, G. L.; Borchardt, R. T.; Rafferty, M. F.; Krass, P. Conformational Preferences of Amphetamine Analogues for Inhibition of Phenylethanolamine *N*-Methyltransferase: Conformationally Defined Adrenergic Agents. 5. *Mol. Pharmacol.* **1981**, *20*, 377–381.
- (34) Wu, Q.; Criscione, K. R.; Grunewald, G. L.; McLeish, M. J. Phenylethanolamine *N*-Methyltransferase Inhibition: Re-evaluation of Kinetic Data. *Bioorg. Med. Chem. Lett.* **2004**, *14*, 4217–4220.
- (35) U'Prichard, D. C.; Greenberg, D. A.; Snyder, S. H. Binding Characteristics of a Radiolabeled Agonist and Antagonist at Central Nervous System Alpha Noradrenergic Receptors. *Mol. Pharmacol.* **1977**, *13*, 454–473.
- (36) Grunewald, G. L.; Romero, F. A.; Seim, M. R.; Criscione, K. R.; Deupree, J. D.; Spackman, C. C.; Bylund, D. B. Exploring the Active Site of Phenylethanolamine *N*-Methyltransferase with 3-Hydroxyethyl- and 3-Hydroxypropyl-7-Substituted-1,2,3,4-tetrahydroisoquinolines. *Bioorg. Med. Chem. Lett.* **2005**, *15*, 1143–1147.
- (37) ClogP values were calculated using the JChem (version 3.1) software package. JCHEM is available from ChemAxon Ltd., Maramaros koz 3/a Budapest 1037, Hungary, <http://www.chemaxon.com>.
- (38) Grunewald, G. L.; Romero, F. A.; Criscione, K. R. Nanomolar Inhibitors of CNS Epinephrine Biosynthesis: (*R*)-(+)-3-Fluoromethyl-7-(*N*-substituted aminosulfonyl)-1,2,3,4-tetrahydroisoquinolines as Potent and Highly Selective Inhibitors of Phenylethanolamine *N*-Methyltransferase. *J. Med. Chem.* **2005**, *48*, 1806–1812.
- (39) Grunewald, G. L.; Romero, F. A.; Chieu, A. D.; Fincham, K. J.; Bhat, S. R.; Criscione, K. R. Exploring the Active Site of Phenylethanolamine *N*-Methyltransferase: 3-Alkyl-7-substituted-1,2,3,4-tetrahydroisoquinoline Inhibitors. *Bioorg. Med. Chem.* **2005**, *13*, 1261–1273.
- (40) Morris, G. M.; Goodsell, D. S.; Halliday, R. S.; Hart, W. E.; Belew, R. K.; Olson, A. J. Automated Docking Using a Lamarckian Genetic Algorithm and an Empirical Binding Free Energy Function. *J. Comput. Chem.* **1998**, *19*, 1639–1662.
- (41) Gee, C. L.; Tyndall, J. D.; Grunewald, G. L.; Wu, Q.; McLeish, M. J.; Martin, J. L. Binding Mode of Methyl Acceptor Substrates to the Adrenaline-Synthesizing Enzyme Phenylethanolamine *N*-Methyltransferase: Implications for Catalysis. *Biochemistry* **2005**, *44*, 16875–16885.
- (42) Brunger, A. T.; Adams, P. D.; Clore, G. M.; DeLano, W. L.; Gros, P.; Grosse-Kunstleve, R. W.; Jiang, J. S.; Kuszewski, J.; Nilges, M.; Pannu, N. S.; Read, R. J.; Rice, L. M.; Simonson, T.; Warren, G. L. Crystallography & NMR System: A New Software Suite for Macromolecular Structure Determination. *Acta Crystallogr., Sect. D* **1998**, *54* (Pt 5), 905–921.
- (43) Jones, T. A.; Zou, J. Y.; Cowan, S. W.; Kjeldgaard, M. Improved Methods for Building Protein Models in Electron Density Maps and the Location of Errors in these Models. *Acta Crystallogr.* **1991**, *A47*, 110–119.
- (44) Schuettelkopf, A. W.; van Aalten, D. M. F. PRODRG—A Tool for High-Throughput Crystallography of Protein–Ligand Complexes. *Acta Crystallogr.* **2004**, *D60*, 1355–1363.
- (45) Kleywegt, G. J.; Jones, T. A. Databases in Protein Crystallography. *Acta Crystallogr.* **1998**, *D54*, 1119–1131.
- (46) Brünger, A. T. Free *R* Value: A Novel Statistical Quantity for Assessing the Accuracy of Crystal Structures. **1992**, *355*, 672–675.
- (47) Grunewald, G. L.; Caldwell, T. M.; Li, Q. F.; Dahanukar, V. H.; McNeil, B.; Criscione, K. R. Enantiospecific Synthesis of 3-Fluoromethyl-, 3-Hydroxymethyl-, and 3-Chloromethyl-1,2,3,4-tetrahydroisoquinolines as Selective Inhibitors of Phenylethanolamine *N*-Methyltransferase versus the α_2 -Adrenoceptor. *J. Med. Chem.* **1999**, *42*, 4351–4361.
- (48) SYBYL 7.0; Tripos, Inc.: 1699 South Hanley Rd., St. Louis, MO 63144, U.S.A.
- (49) Sall, D. J.; Grunewald, G. L. Inhibition of Phenylethanolamine *N*-Methyltransferase (PNMT) by Aromatic Hydroxy-Substituted 1,2,3,4-Tetrahydroisoquinolines: Further Studies on the Hydrophilic Pocket of the Aromatic Ring Binding Region of the Active Site. *J. Med. Chem.* **1987**, *30*, 2208–2216.

JM060466D